Journal of Pharmaceutical Analysis 2014;4(3):173–182

Contents lists available at ScienceDirect

Journal of Pharmaceutical Analysis

www.elsevier.com/locate/jpa
www.sciencedirect.com

ORIGINAL ARTICLE

Derringer desirability and kinetic plot LC-column comparison approach for MS-compatible lipopeptide analysis

Matthias D'Hondt, Frederick Verbeke, Sofie Stalmans, Bert Gevaert, Evelien Wynendaele, Bart De Spiegeleer*

Drug Quality and Registration (DruQuaR) Group, Faculty of Pharmaceutical Sciences, Ghent University, Harelbekestraat 72, B-9000 Ghent, Belgium

Received 6 February 2013; accepted 9 September 2013
Available online 18 September 2013

KEYWORDS

Lipopeptide;
Hierarchical cluster analysis (HCA);
Principal component analysis (PCA);
LC–MS;
Kinetic plot;
Derringer desirability function

Abstract Lipopeptides are currently re-emerging as an interesting subgroup in the peptide research field, having historical applications as antibacterial and antifungal agents and new potential applications as antiviral, antitumor, immune-modulating and cell-penetrating compounds. However, due to their specific structure, chromatographic analysis often requires special buffer systems or the use of trifluoroacetic acid, limiting mass spectrometry detection. Therefore, we used a traditional aqueous/acetonitrile based gradient system, containing 0.1% (m/v) formic acid, to separate four pharmaceutically relevant lipopeptides (polymyxin B_1, caspofungin, daptomycin and gramicidin A_1), which were selected based upon hierarchical cluster analysis (HCA) and principal component analysis (PCA).

In total, the performance of four different C18 columns, including one UPLC column, were evaluated using two parallel approaches. First, a Derringer desirability function was used, whereby six single and multiple chromatographic response values were rescaled into one overall *D*-value per column. Using this approach, the YMC Pack Pro C18 column was ranked as the best column for general MS-compatible lipopeptide separation. Secondly, the kinetic plot approach was used to compare the different columns at different flow rate ranges. As the optimal kinetic column performance is obtained at its maximal pressure, the length elongation factor λ (P_{max}/P_{exp}) was used to transform the obtained experimental data (retention times and peak capacities) and construct kinetic performance limit (KPL) curves, allowing a direct visual and unbiased comparison of the selected columns, whereby the YMC Triart C18 UPLC and ACE C18

*Corresponding author. Tel.: +32 9 264 81 00; fax: +32 9 264 81 93.
E-mail address: Bart.DeSpiegeleer@UGent.be (B. De Spiegeleer).
Peer review under responsibility of Xi'an Jiaotong University.

Production and hosting by Elsevier

http://dx.doi.org/10.1016/j.jpha.2013.09.001

columns performed as best. Finally, differences in column performance and the (dis)advantages of both approaches are discussed.

1. Introduction

As can be derived from the name, lipopeptides differ from ordinary peptides in the connection of an acyl chain to a linear or cyclic (oligo) peptide structure, resulting in amphiphilic properties [1]. Natural lipopeptides originate mostly from a bacterial or fungal origin, in which *Pseudomonas* and *Bacillus* species have been studied extensively. Certain lipopeptide compounds exert an antibacterial function through pore formation in membranes, resulting in bacterial death. Currently, they are used as a last line of defense in treatment of infections caused by multidrug-resistant organisms. Other lipopeptides block the 1–3-β-glucan synthase enzyme, which results in a fungicidal activity due to loss of cell wall integrity [2–13]. Moreover, some lipopeptides have known antiviral and antitumor, as well as immune-modulating properties through Toll-like receptors [14–17]. Currently, lipopeptides are also under investigation to be applied as cell-penetrating peptides (CPP). The addition of an acyl chain to cell-penetrating peptides generally enhance the penetration efficiency of these components, allowing transport of short oligonucleotides (DNA, RNA), plasmid DNA and proteins into the cell, rendering them a promising class of non-viral delivery vectors [18–20]. Lipopeptides are also important chemical compounds in the quorum sensing mechanisms between bacteria, playing a role in *i.a.,* biofilm formation [21–24].

Lipopeptides are thus becoming an increasingly important subgroup of peptides, attracting more and more pharmaceutical and biomedical attention. However, due to their specific structure, chromatographic analysis often requires the use of special buffer systems, *e.g.*, sodium sulfate [25–28] or trifluoroacetic acid [29–32]. These systems are not directly compatible with mass spectrometry or can cause quantification problems due to ion suppression [33]. Therefore, the goal of this study was to define the best LC–MS compatible system for general lipopeptide analysis, using a formic acid containing water/acetonitrile based gradient. Samples possibly containing new, undiscovered, bioactive lipopeptides can be screened by this new (U)HPLC–MS method. Therefore, the main focus point of this article was the separation of different lipopeptide classes, representing the majority of the lipopeptide chemical space. To achieve this, we have first selected a number of model lipopeptides from a list of 22 pharmaceutically relevant lipopeptides (Table 1), using their chemical descriptors and applying clustering techniques (HCA and PCA).

The four LC columns were selected based on their pharmacopoeial and general use in lipopeptide analysis. Column comparison was performed using two parallel approaches. First, using similar chromatographic conditions, the performance was evaluated and ranked using a Derringer desirability function, combining six individual chromatographic responses, each given the same weight, *i.e.*, asymmetry factor, limit of detection (LOD), time-corrected resolution product, separation factor, peak capacity and chromatographic response factor [34]. Secondly, the kinetic plot approach is based on the principle that the kinetic optimum of a chromatographic system or column is achieved when a preset desired efficiency or peak capacity is reached in the shortest possible time frame or alternatively, when a maximum efficiency is reached during a preset time frame. Therefore, a plot of the analysis time *vs.* the plate number (isocratic) or peak capacity (gradient) provides the most direct way to compare the performance of chromatographic systems with different physicochemical properties. As this kinetic optimum is always obtained when the chromatographic system is operated at its maximal pressure, the different columns are therefore compared on an unbiased basis, *i.e.*, preventing that one column is tested under less than optimal conditions [35–40]. Finally, both approaches are compared.

2. Materials and methods

2.1. Materials

Polymyxin B sulfate (Ph. Eur. quality [27]) was bought at Genaxxon BioScience (Ulm, Germany). Gramicidin A (>90% purity) and formic acid (MS grade >98%) were obtained from Sigma Aldrich (Bornem, Belgium). Cubicin® (containing 94.6% (w/w) daptomycin—Novartis) and Cancidas® (containing 41.7% (w/w) caspofungin—MSD) were purchased from Care4Pharma (Schiphol, The Netherlands). Acetonitrile (LC–MS grade) was purchased from Fisher Scientific (Aalst, Belgium). Water was purified using an Arium 611 purification system (Sartorius, Gottingen, Germany) yielding ≥ 18.2 MΩ cm quality

Table 1 Lipopeptide selection.

#	Compound	Formula	M_r[a]	Ref.
1	Amphomycin	$C_{58}H_{91}N_{13}O_{20}$	1290.42	[2]
2	Anidulafungin	$C_{58}H_{73}N_7O_{17}$	1140.24	[2]
3	Arthrofactin	$C_{64}H_{111}N_{11}O_{20}$	1354.63	[5]
4	**Caspofungin**	**$C_{52}H_{88}N_{10}O_{15}$**	**1093.31**	**[2]**
5	Cilofungin	$C_{49}H_{71}N_7O_{17}$	1030.12	[6]
6	Colistin A	$C_{53}H_{100}N_{16}O_{13}$	1169.46	[2]
7	Colistin B	$C_{52}H_{98}N_{16}O_{13}$	1155.43	[2]
8	Dalbavancin	$C_{88}H_{100}Cl_2N_{10}O_{28}$	1816.69	[2]
9	**Daptomycin**	**$C_{72}H_{101}N_{17}O_{26}$**	**1620.67**	**[2]**
10	Echinocandin B	$C_{52}H_{81}N_7O_{16}$	1060.24	[2]
11	**Gramicidin A_1**	**$C_{99}H_{140}N_{20}O_{17}$**	**1882.29**	**[7]**
12	Iturin A_2	$C_{48}H_{74}N_{12}O_{14}$	1043.17	[8]
13	Micafungin	$C_{56}H_{71}N_9O_{23}S$	1270.27	[2]
14	MX-2401	$C_{67}H_{101}N_{15}O_{22}$	1468.61	[2]
15	P_3CSS	$C_{60}H_{113}N_3O_{11}S$	1084.62	[9]
16	Plipastatin	$C_{72}H_{110}N_{12}O_{20}$	1463.71	[10]
17	**Polymyxin B_1**	**$C_{56}H_{98}N_{16}O_{13}$**	**1203.48**	**[2]**
18	Ramoplanin A_2	$C_{119}H_{154}N_{21}O_{40}$	2554.07	[11]
19	Surfactin	$C_{53}H_{93}N_7O_{13}$	1036.34	[10]
20	Syringomycin E	$C_{53}H_{85}ClN_{14}O_{17}$	1225.78	[12]
21	Teicoplanin A2-2	$C_{88}H_{97}ClN_{12}O_{33}$	1879.66	[13]
22	Telavancin	$C_{80}H_{106}Cl_2N_{11}O_{27}P$	1755.64	[2]

Bold: selected lipopeptides based upon PCA and HCA.
[a]Calculated values using MarvinSketch software (version 5.4.1.1, ChemAxon Ltd.).

water. YMC Pack Pro C18, YMC Triart C18 HPLC, ACE C18 (all 250 mm × 4.6 mm I.D.; 5 µm particle size) and YMC Triart C18 UPLC (100 mm × 2.0 mm I.D.; 1.9 µm particle size) columns were obtained from Achrom (Machelen, Belgium).

2.2. *Lipopeptide clustering*

The molecular structures of 22 pharmaceutically relevant lipopeptides in isomeric SMILES format [41], were imported into MarvinSketch (version 5.4.1.1, ChemAxon Ltd.), thus obtaining a two-dimensional peptide model. The selection was based upon (i) clinical application as antibacterial agent (*e.g.*, polymyxin B sulfate), antifungal agent (*e.g.*, anidulafungin) or adjuvant (*e.g.*, P_3CSS) and (ii) prior use in biomedical research, *i.e.*, new potential APIs (*e.g.*, MX-2401). As some lipopeptides consisted of mixtures of closely related compounds (*e.g.*, polymyxin B_1, $B_{1\text{-}I}$, B_2 and B_3), the structures of the main compound (*e.g.*, polymyxin B_1) were considered in this study. Gramicidin A_1, although strictly speaking not a lipopeptide, was also included in this set of 22, based upon its similar antibacterial working mechanism (*i.e.*, pore formation in bacterial cell wall) and its deviating structure as it does not contain the typical conjugated acyl chain present in the other selected lipopeptides, but rather a series of hydrophobic amino residues (alanine, valine and leucine). Structural information of the 22 lipopeptides used in this clustering is given in Supplementary Data.

Three-dimensional structure optimization was performed using HyperChem 8.0 (Hypercube, Gainesville, FL, USA) software. The molecular mechanics force field method using the Polak–Ribière conjugate gradient algorithm, with a root mean square (RMS) of 0.1 kcal/(Å mol) as termination condition, was used. Using the 3-D optimized lipopeptide structures, 3224 descriptors were calculated using Dragon (version 5.5, Talete), 5 descriptors were calculated using MarvinSketch software (pI and Log *D* at pH 2.0, 5.5, 7.4 and 10.0) and 7 descriptors were calculated using the HyperChem software [42]: the solvent accessible Surface Area (i, ii) was computed using both the fast approximate method and a more accurate grid algorithm. The lipopeptide Volume (iii) calculation also employed this grid algorithm. The calculation of the Hydration Energy (iv), which determines the stability of the molecular conformation, was based on the exposed surface area. Log *P* (v) and Refractivity (vi) values were estimated by the Ghose, Pritchett and Crippen approach, whereby each atom contributes to the overall hydrophobicity and refractivity, respectively. Finally, Polarizability (vii) was calculated based upon different increments associated with the different atom types. In total, 3236 descriptors were obtained for each lipopeptide.

Elimination of constant descriptors, *i.e.*, identical value for all lipopeptides, reduced the number of descriptors to 1464. Each descriptor data set was then transformed into a *N* (0,1) distribution using *z*-score normalization

$$z = \frac{x - \overline{X}}{SD}$$

where, *x* is the individual value of a data point, $\overline{X}$ is the mean and *SD* is the standard deviation of the descriptor data set.

Lipopeptide clustering was performed using HCA analysis with SPSS software (SPSS 19, IBM) and PCA with SIMCA-P+ software (version 12.0, Umetrics). The HCA is used for pattern recognition based on similarities between objects according to the Euclidean distance and the result is visualized in a dendrogram. Starting from the individual components, branches are built up to form clusters. The length of the branches are inversely related to their similarity, thus short branches mean high similarity. PCA is a tool for the interpretation of large data tables and visualization of systematic trends. In this approach the multidimensional space, characterized by the 1464 descriptor variables, is reduced to principal components (PC), which are linear combinations of the original variables, whereby the first PC withholds the most variability in the data set. Based on commercial availability, a lipopeptide representative for each of the formed clusters was used for further column comparison.

2.3. *Column selection*

Four different stationary phases were evaluated for lipopeptide separation. The YMC Pack Pro C18 column (V_c: 2.125 mL) was selected based on the work of Orwa et al. [26], where this column showed the best chromatographic separation of the different polymyxin B sulfate constituents. The second and third columns, *i.e.*, the YMC Triart C18, have comparable hydrophobicity k' (amylbenzene) value as the YMC Pack Pro C18 column (both approximately 7.0), but have a 20% lower hydrogen bonding capacity α (caffeine/benzene) due to a multi-stage endcapping procedure of the residual silanol groups (the YMC Pack Pro C18: 0.105 *vs.* 0.085 for the YMC Triart C18 chemistry) [43]. This stationary phase was obtained both in HPLC (V_c: 2.082 mL) and UPLC (V_c: 0.438 mL) compatible format, of which the latter, due to lower particle size (1.9 µm), has the additional benefit of its ultra-fast analysis time. The last column, *i.e.*, ACE C18 (V_c: 1.968 mL) was selected based on a column comparison which indicated better peak shape and column efficiency when compared to the YMC Pack Pro C18 column for basic compounds, while the hydrophobicity and selectivity are very close to the YMC Pack Pro C18 stationary phase [44].

2.4. *Chromatography*

The UPLC apparatus consisted of a Waters Acquity H UPLC Class Quaternary Solvent Manager, a Waters Acquity Sample Manager, combined with a Flow Through Needle, and a Waters Acquity Ultra Performance LC PDA (500 nL–10 mm path length analytical flow cell) detector, with Empower 2 software for data acquisition. Mobile phases consisted of 0.1% (m/v) formic acid in water (A) and 0.1% (m/v) formic acid in acetonitrile (B). A general linear gradient was implemented running from 10% B to 90% B in 25 column volumes (V_c) followed by returning to the initial conditions and re-equilibration. A lipopeptide mixture sample containing 0.1 mg/mL polymyxin B sulfate, gramicidin A, daptomycin and 1.0 mg/mL caspofungin was prepared in H_2O/ACN (50:50, v/v) containing 0.1% formic acid. Higher concentrations exceeded the solubility, yielding a turbid solution. Column temperature was set at 40 °C (±5 °C) and sample compartment at 5 °C (±3 °C). The injection volumes for the HPLC and UPLC column analysis were set at 10 µL and 2 µL, respectively. UV-detection was performed at 215 nm, using a sampling rate of 20 Hz combined with a detector time constant of 0.1 s. The flow rates for the Derringer comparison were set at 1.0 and 0.5 mL/min for the HPLC and the UPLC columns, respectively. The flow rate settings used in the kinetic plot approach are discussed in detail in Section 2.6. As mentioned in Section 2.2, only the major constituent of the individual lipopeptide (*i.e.*, polymyxin B_1 in the

polymyxin B sulfate and gramicidin A_1 in gramicidin A) was considered, as the main objective was to evaluate the separation between structurally different lipopeptides, rather than between the closely related ones.

2.5. Derringer comparison—chromatographic response factors

The lipopeptide chromatographic characteristics were divided into six different response factors, containing both single and multiple responses, and are presented in Table 2 [27,45,46]. As four lipopeptides were analyzed on each column, 3–4 separate values for certain single responses, *i.e.*, separation factor (S) and asymmetry factor (A_s), were obtained per column. These separate values of these single responses, as well as the multiple responses, were re-expressed as a dimensionless desirability scale (d) using two linear desirability functions, depending on whether the desired chromatographic response was to be minimized, *e.g.*, LOD, or maximized, *e.g.*, peak capacity. The geometrical mean of the aforementioned separate d-values of the single responses was calculated to obtain one average d-value for the single response per column. Finally, the geometrical mean of the six d-values was calculated in order to assess the overall performance (D-value) of each column [34,46], thereby appointing equal weights to each of the six response factors.

$$\text{Minimized}: d(Y) = \frac{1.1Y_{\max} - Y_i}{1.1Y_{\max} - 0.9Y_{\min}}$$

$$\text{Maximized}: d(Y) = \frac{Y_i - 0.9Y_{\min}}{1.1Y_{\max} - 0.9Y_{\min}}$$

$$\text{Desirability function}: D = \left(\prod_{i=1}^{x} d_i\right)^{1/x}$$

In which d is the desirability value, D is the geometric mean of the desirability values, Y_i are the experimental response value and $Y_{\min}$ and $Y_{\max}$ are the minimal and maximum values within the experimental data set.

2.6. Kinetic plots

Kinetic performance limit (KPL)-curves were constructed for each column by performing the experiments described in Section 2.4 at different flow rates, whereby the total gradient time was adjusted accordingly, *i.e.*, fixed at 25 V_c, in order to conserve equal gradient steepness. For each individual column experiment at a given flow rate, the corresponding peak capacity $n_{p,\exp}$ was calculated (Table 2). These experimental peak capacities $n_{p,\exp}$, as well as the retention times (T_R) of the last eluting lipopeptide, *i.e.*, gramicidin, were subsequently converted into KPL-data points, (*i.e.,* $n_{p,\mathrm{KPL}}$ and $T_{R,\mathrm{KPL}}$) using the length elongation factor λ:

$$\lambda = \frac{P_{\max}}{P_{\exp}}$$

where $P_{\max}$ is the maximum allowed column or system pressure and $P_{\exp}$ is the maximum pressure achieved during the chromatographic analyses.

$$n_{p,\mathrm{KPL}} = 1 + \sqrt{\lambda} \times (n_{\mathrm{p}} - 1)$$

$$T_{R,\mathrm{KPL}} = \lambda T_{\mathrm{R}}$$

To determine the flow rate range to be used within the kinetic plot experiments, the highest flow rates, resulting in a still acceptable $P_{\exp}$ column pressure were determined for the four selected (U)HPCL columns. The lowest flow rates were determined in reference to the fixed flow rates used during the Derringer column comparison. Thus, the flow rate ranges used for the kinetic plot evaluation of the HPLC and UPLC columns were 0.60–1.40 mL/min and 0.20–0.80 mL/min, respectively, with 7 different rates per column. Subsequently, each of the 7 obtained data points per column was plotted ($T_{R,\mathrm{KPL}}$ in function of $n_{p,\mathrm{KPL}}$) to obtain the KPL-curve [35–40].

Table 2 Selected chromatographic response factors and formulas.

#	Response factor	Formula	#[a]
1	Asymmetry factor (A_s)	$A_s = \frac{w_{0.05}}{2d}$	4
2	Limit of detection (LOD) (ng)	$\frac{S}{N} = \frac{2H}{h} = 3$	4
3	Time-corrected resolution product ($R_{s\ \mathrm{corr}}$)	$R_s = \frac{1.18(t_{R2} - t_{R1})}{w_{h1} + w_{h2}}$ $\prod R_{s\ \mathrm{corr}} = \frac{\prod R_s}{T_{R\max}}$	1
4	Separation factor (S)	$S = \frac{t_{R2} - t_0}{t_{R1} - t_0}$	3
5	Peak capacity (n_p)	$n_p = 1 + \frac{t_g}{1/n(\sum_1^n w_h)}$	1
6	Chromatographic response function (CRF)	$CRF = a\sum_{i=1}^{n-1} R_{s\ i,\ i+1} + b(t_g - R_{T\max})$	1

$w_{0.05}$: peak width at one-twentieth of the peak height.
w_h: width of the peak at half-height.
d: distance between the perpendicular dropped from the peak maximum and the leading edge of the peak at one-twentieth of the peak height.
H: height of the peak.
h: range of the noise.
t_R: retention time of the peak corresponding to the component.
t_0: column dead time.
$R_{T\max}$: t_0-corrected t_R of the last peak, expressed as column volume.
t_g: defined gradient run time expressed in column volume.
a: 1.
b: 1.
[a]Number of responses obtained per column.

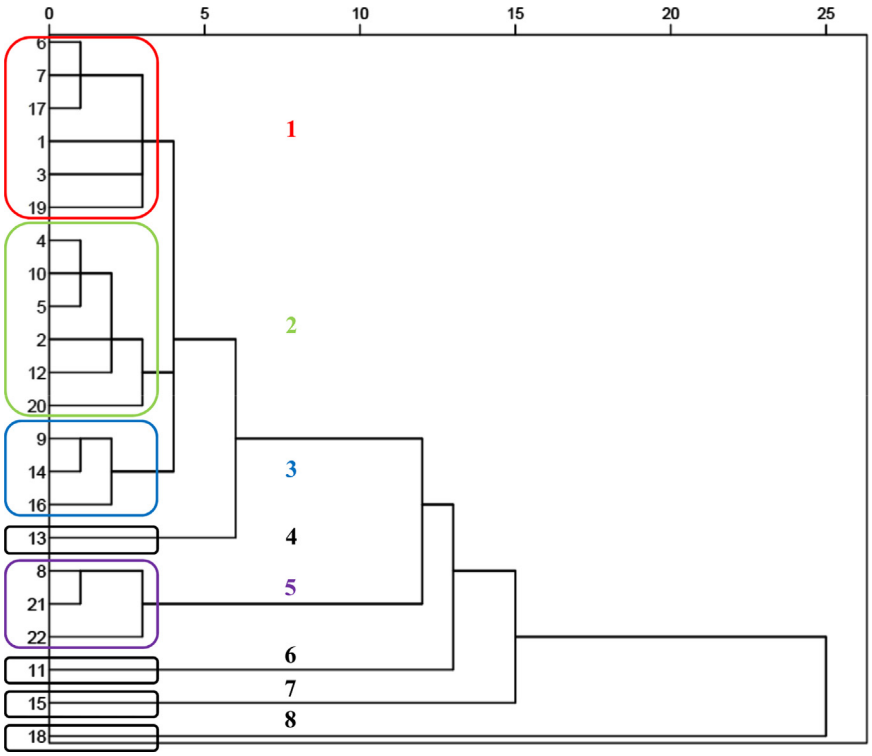

Fig. 1 Dendrogram obtained from hierarchical cluster analysis of 22 lipopeptides.

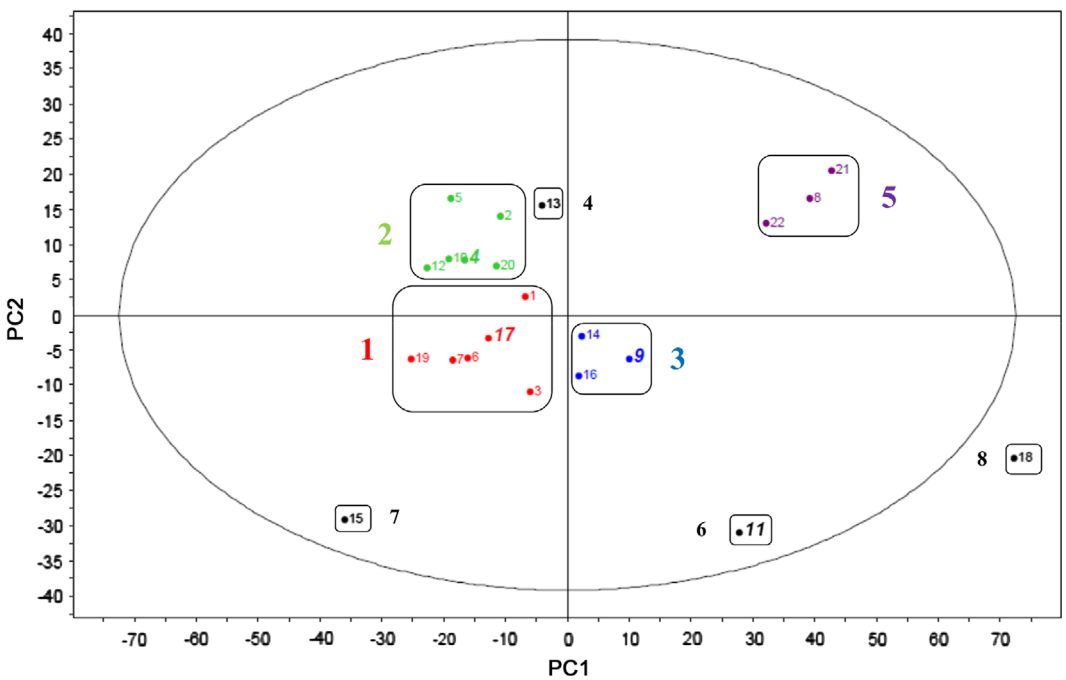

Fig. 2 Principal component analysis score plot (PC1–PC2) for the 22 lipopeptides.

3. Results and discussion

3.1. *Lipopeptide clustering*

The resulting dendrogram of the HCA and the results of the PCA, visualized by means of score plots, are shown in Figs. 1 and 2. The first four PCs explained approximately 80% of the structural variability of the 22 selected lipopeptides.

Based on the PCA result (Fig. 2), we can see that peptides 15, 11 and 18 (clusters 6, 7 and 8), and to a lesser extent, components 22, 8 and 21 ('violet' cluster 5), are very dissimilar to all other components which are classified into three major clusters (red, green and blue

clusters, 1–3) and a fourth cluster containing micafungin (13). This can also be observed in the HCA dendrogram (Fig. 1, similar color legend). The major lipopeptide cluster, containing 72% of the originally selected lipopeptides, includes compounds adhering to the most strict lipopeptide definition, *i.e.*, direct connection of an acyl chain to a linear or cyclic (oligo)peptide structure. As previously mentioned, this major cluster can be divided into four sub-clusters, thus classifying the original 22 components into 8 clusters. The other, structurally deviating lipopeptides still contain the connection of an acyl chain to a linear or cyclic (oligo)peptide structure, but also include sugar residues (ramoplanin—peptide 18), multiple lipid chains (P_3CSS—peptide 15) or alternative linkage between acyl chain and peptide structure (cluster 5, peptides 8, 21 and 22) in their structures (Supplementary Data). Gramicidin (peptide 11) does not contain the typical conjugated acyl chain present in the other selected lipopeptides, but rather a series of hydrophobic amino residues (alanine, valine and leucine).

Based on commercial availability, lipopeptide representatives, *i.e.*, polymyxin B_1 (17, belonging to the red cluster 1), caspofungin (4, green cluster 2), daptomycin (9, blue cluster 3) and gramicidin A_1 (11, cluster 6) were selected, thus representing the major lipopeptide cluster as well as one structurally different cluster.

3.2. *Chromatographic response factors—Derringer comparison*

The chromatographic responses, together with their calculated *d*-values and overall *D*-value, are presented in Table 3. The chromatograms obtained using the four different columns are depicted in Fig. 3.

The average lipopeptide asymmetry factor, calculated using the four individual A_s of the lipopeptides, showed large variability (average 81% RSD) on each of the selected columns, which can be explained by the fact that the four lipopeptides were selected based on their structural diversity, resulting in different interactions with the stationary phase. The best A_s results, *i.e.*, closest to 1 for the 4 lipopeptides, were obtained with the YMC Pack Pro C18 column (average A_s: 1.16, 45% RSD), suggesting a more uniform lipopeptide column interaction. Alternatively, the average asymmetry factor of the individual lipopeptides on the four different columns showed a smaller variability (average 38% RSD), which can be explained by the different endcapping procedures/efficiencies leading to different amounts of peak tailing. However, Grubbs outlier testing (α: 0.05) showed no outliers in the individual lipopeptide asymmetry factors, indicating that the individual lipopeptides interacted in a similar way with all of the four selected stationary phases.

Table 3 Chromatographic response values, calculated desirability values (*d*) and overall desirability values (*D*).

Parameter	ACE C18	YMC Pack Pro C18	YMC Triart C18 HPLC	YMC Triart C18 UPLC
A_s	3.783	**1.160**	1.912	2.343
d	0.529	**0.658**	0.262	0.247
LOD[a]	14.605	56.822	29.381	**3.064**
d	0.725	0.239	0.248	**0.991**
$R_{s\ corr}$	250.96	**1350.88**	153.10	69.91
d	0.132	**0.905**	0.063	0.005
S	1.335	**2.188**	1.805	1.574
d	0.428	**0.807**	0.469	0.287
n_p	**180.400**	172.931	142.927	113.523
d	**0.813**	0.735	0.423	0.118
CRF	70.182	**97.984**	58.519	47.853
d	0.419	**0.849**	0.239	0.074
D	0.441	**0.644**	0.241	0.120

Bold: best chromatographic response/highest *d* or *D* value.
[a]Absolute mass on column (ng).

The LOD is the smallest amount of substance that is accurately detectable, having a S/N ratio of 3. Both the signal or peak height, which can be correlated to the 'sharpness' of the peak, and the amount of noise determine the LOD value. The average noise value obtained with the four columns is calculated to be 2.121×10^{-4} AU (22.03% RSD). On the other hand, the peak heights of the individual lipopeptides were seen to differ between the selected columns (Fig. 3). This peak height is directly proportionate to the detectors ability of detecting the solute concentration at the maximum of the peak (C_{max}). As all analyses were performed using the same chromatographic system (incl. tubings, injector and detector), any observed peak broadening, resulting in decrease in peak height, can be attributed to the analytical column. Moreover, peak areas of the four lipopeptides analyzed on the three HPLC columns were found to be similar (%RSD ranging from 1.22 to 8.11).

The relationship between the C_{max} and the column parameters is summarized in following formula [47]:

$$C_{max} = \frac{4}{\varepsilon_t \pi \sqrt{2\pi}(1 + |A_s - 1|)} \times \frac{\sqrt{N}}{L d_c^2} \times \frac{V_0 C_0}{(1 + k')}$$

Derivation of the formula is thoroughly discussed in Supplementary Data. In this formula, the first term includes the column porosities (ε_t), which were found to be similar throughout the four columns. This term also corrects the Gaussian peak profile for the any peak asymmetries, both fronting and tailing. As the average asymmetry factors ranged from 1.16 to 3.78, this will have a significant influence on the LOD (Table 3).

The second term incorporates the column efficiency (*N*) and the column dimensions, *i.e.*, length (*L*) and diameter (d_c). On its own, *N* is influenced by column length (*L*) and particle size (d_p) ($N \sim L/d_p$). When comparing the HPLC and UPLC columns, *L* is reduced from 250 to 100 mm, and the d_p is reduced from 5 μm to 1.9 μm, resulting in a near constant L/d_p ratio of 50,000 for both column dimensions (*i.e.,* $250,000\ \mu m/5\ \mu m$ (HPLC) $\approx 100,000\ \mu m/1.9\ \mu m$ (UPLC)). However, the reduction in column dimensions, *i.e.*, *L* (250–100 mm) and d_c (4.6–2.0 mm), will increase the C_{max} result and thus the peak height.

The third and final term, links the C_{max} to the absolute mass loaded onto the column, *i.e.*, injection volume (v_0) and concentration (c_0), as well as to the retention characteristics (k'). As c_0 is constant, the absolute mass loaded onto the HPLC column is 5 times higher than the mass injected onto the UPLC column (10 *vs.* 2 μL v_0). However, as the LOD is expressed as absolute mass, the calculations already accounted for this difference in absolute mass loaded onto the UPLC column (see Supplementary Data). It also takes into account the capacity factor, which do not differ significantly throughout the four columns (% RSD of the lipopeptide k' values on the four different columns range from 21% to 50%).

When summarizing these different LOD influences, *i.e.*, reduction of column length, column diameter and peak asymmetry factor, the YMC Triart C18 UPLC peak height will be approximately 11 times higher as the peak height obtained using the YMC Triart C18 HPLC column when identical quantities (mass) are injected. Indeed, the LOD results for the YMC Triart C18 HPLC and UPLC columns, *i.e.*, 29 and 3 ng respectively, demonstrate this underlying relationship, as their LOD values differ by approximately a factor 10.

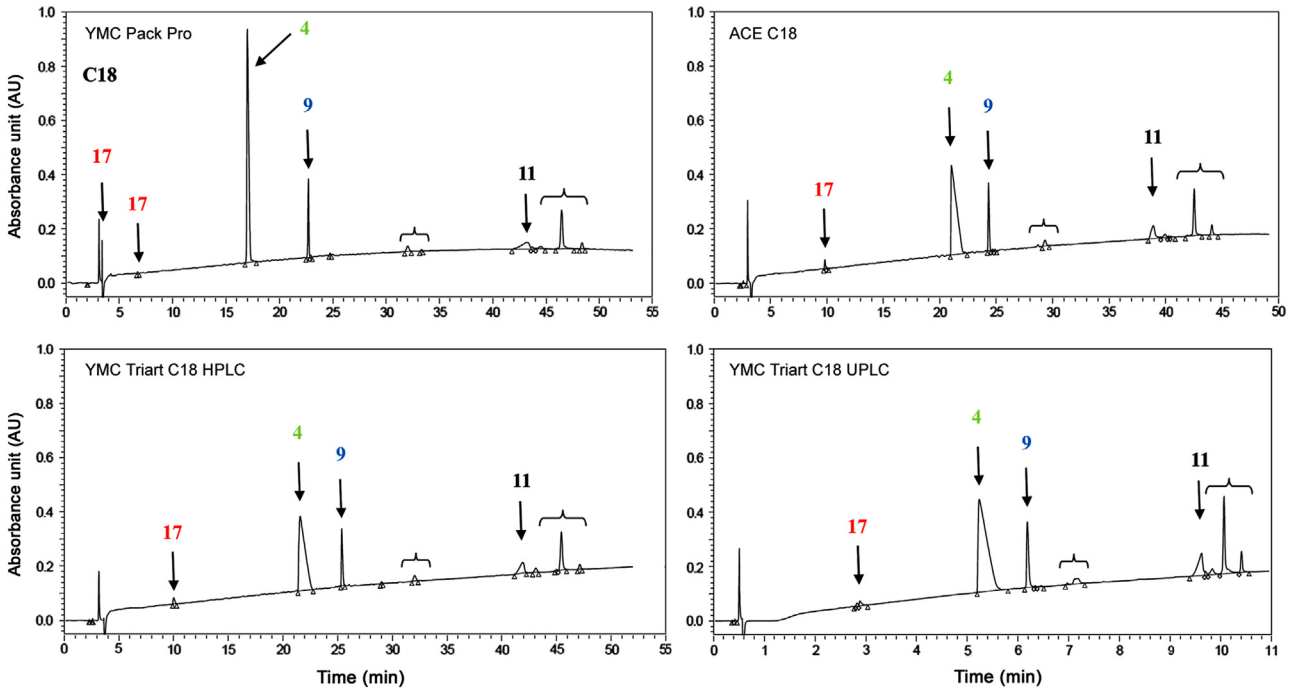

Fig. 3 Typical chromatograms obtained during the Derringer column comparison. The *X*-axis was fixed at 25 column volumes. Peaks indicated by arrow are the selected lipopeptides (left to right: polymyxin B_1 (17), caspofungin (4), daptomycin (9) and gramicidin A_1 (11)); peaks indicated by braces are considered blank peaks.

The high LOD value observed when using the YMC Pack Pro C18 column is caused by an unretained fraction of the injected polymyxin B_1, causing a smaller retained polymyxin B_1 peak (*i.e.*, smaller *S* value), leading to a relative high LOD value for polymyxin, which in turn leads to a higher average LOD value for the four lipopeptides, and smaller LOD *d*-value for the YMC Pack Pro C18 column. The presence of polymyxin B_1 compounds in the unretained peak was verified using mass spectrometry (MS^1 and MS^2). Different factors (polymyxin B_1 concentration, column temperature, gradient composition, column batch and sample solvent strength) were varied to investigate their influence on this peculiar polymyxin B_1 retention pattern. The main cause of this observed dual retention, which is influenced by a variety of parameters, is the strength of the sample solvent in relationship to the starting strength of the applied gradient. As the sample, dissolved in 50/50 H_2O/ACN sample solvent, is injected onto the column, two processes occur. (i) A plug containing the strong sample solvent will move unretained through the column, and due to its strong solvent strength above the critical value for desorption, will cause the polymyxin B_1 to remain in this plug, desorbed from the stationary phase. (ii) While moving through the column, there is a diffusion of polymyxin B_1 from this plug into the mobile phase. In this mobile phase, polymyxin B_1 adsorbs to the hydrophobic surface of the stationary phase, and remains adsorbed until the concentration of acetonitrile in the gradient reaches the critical value necessary to cause sudden desorption from the stationary phase. The diffusion process of polymyxin B_1 from the plug into the mobile phase, and from there adsorption to the stationary phase, occurs continuously whilst the plug is moving through the column. This polymyxin B_1 diffusion into the mobile phase occurs throughout the entire column length, resulting in polymyxin B_1 being retained throughout the entire column length, until the gradient at the right solvent strength (*i.e.*, critical value) sweeps away all desorbed polymyxin.

The resolution (R_s) takes into account three key factors: (i) column efficiency (*N*), (ii) selectivity (α) and (iii) retention factor (*k*). As mentioned above, *N* is determined by the column length and particle size and as the L/d_p ratios between the evaluated HPLC and UPLC columns are constant, *N* will not have an influence on the calculated R_s values. Selectivity (k_1/k_2) and retention factors ($(T_R - T_0)/T_0$) are closely related and are determined by mobile phase composition, which was equal for all columns evaluated, and by stationary phase. All columns are based upon the same main separation principle, *i.e.*, reversed-phase C18. Therefore, no major selectivity differences, *e.g.*, different elution orders, were observed for the four lipopeptides. However, subtle difference in stationary phase chemistries between the YMC Pack Pro C18 and the other columns, also reflected in other chromatographic parameters, resulted in higher selectivity values (*e.g.*, YMC Pack Pro C18 *vs.* ACE C18: 1.38 *vs.* 1.18 for α (daptomycin/caspofungin)) and subsequently higher R_s values. The three individual R_s values, obtained for each column, are recalculated into the time corrected resolution product ($R_{s\ corr}$), which also takes the column dead volume corrected retention time (expressed in column volume) of the last eluting lipopeptide in the mixture, *i.e.*, gramicidin A_1, into account. This R_{Tmax} was similar for all columns, *i.e.*, 19.53 V_c (5.69% RSD). Calculation of the separation factor *S*, only takes the column dead volume corrected T_R of the eluting components into account. The YMC Pack Pro column performed the best. The average separation factors of the other three columns showed high similarity, as was also noticed for $R_{s\ corr}$ parameter.

Peak capacity is determined by the total gradient run time and by the individual peak widths at half maximum. The total gradient

run time (expressed as column volumes) is equal to 25 for all columns. Therefore, the peak capacity, as calculated here, can be correlated with the individual peak widths at half maximum. The ACE C18 column performed best, closely followed by the YMC Pack Pro C18 column. The chromatographic response factor takes into calculation the three resolution results obtained for each column and the retention time of the last eluting peak. The YMC Pack Pro C18 column showed the highest CRF value, which is to be expected as the column was also characterized by the highest resolution values. The other three columns showed a comparable, but statistically significant, lower CRF value.

From the global desirability *D*-value, the YMC Pack Pro C18 column showed the best overall performance in the chromatographic characteristics of pharmaceutically important lipopeptides. However, a major drawback of this column was the observation of an unretained fraction of polymyxin B_1. The ACE C18 column ranked as the second best column and the overall performance of the YMC Triart C18 columns, both HPLC and UPLC, were found to be rather similar (Table 3).

3.3. *Kinetic plots*

The four constructed KPL-curves are depicted in Fig. 4. From the extreme $T_{R,KPL}$ points, it can be derived that the YMC Triart C18 UPLC outperforms the three other columns in minimal analysis time. Due to its nature, *i.e.*, smaller void volume and particle size together with higher maximal pressure limit, this UPLC column is able to generate $T_{R,KPL}$ values below 20 min. This T_R region is inaccessible by the HPLC columns, as the maximal applicable column pressure would be exceeded.

The highest column performance was obtained with the ACE C18 and YMC Pack Pro C18 columns, *i.e.*, $n_{p,KPL}$ values of 288 and 284, respectively. As the only variable in the n_p calculation is the peak-width at half-height, as T_g is constant, *i.e.*, 25 V_c for each column, one can expect that a UPLC column will generally result in smaller, sharper peaks compared to an HPLC column, if the sample amount is proportional among both. However, the mean peak width at half-height (expressed in column volumes) using the UPLC column is larger than those obtained with the HPLC columns (0.90 *vs.* 0.56 for ACE C18 and YMC Pack Pro C18). Even the elongation factor λ, which is by far the largest for the UPLC column (4.0 *vs.* 2.5 for the ACE C18) cannot compensate for this mean peak width difference, thus explaining this observation.

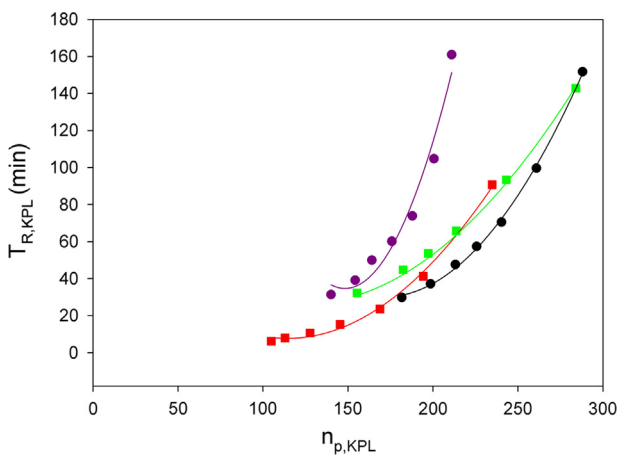

Fig. 4 Kinetic plot with ■ YMC Triart C18 (UPLC); ● ACE C18; ■ YMC Pack Pro C18; ● YMC Triart C18 (HPLC).

3.4. *Comparison of the Derringer desirability vs. kinetic plot approach*

The KPL-curve depicted in Fig. 4 is based on only three variable parameters, *i.e.*, $T_{R,KPL}$, $n_{p,KPL}$ and λ and allows a fast and visual interpretation of column performances. Alternatively, the Derringer desirability function approach is based on using six chromatographic responses, including the experimentally obtained n_p, which allows a more exhaustive comparison of the selected columns. Moreover, certain chromatographic responses can be emphasized in the Derringer desirability approach by assigning certain weight factors. However, the Derringer approach also increases the overall data processing and interpretation time. Chromatography of the components can be adjusted by fine-tuning either the physical or the chemical column properties. Regarding the comparison of chemical properties and the interaction between the analytes and chromatographic system, the Derringer desirability function outperforms the kinetic plot method. For example, peak tailing is related to the chemical properties of the stationary phase, thus providing initial information of the column chemistry, which is lacking in the kinetic plot method. Although the retention time of a compound on a given column is also related to the column chemistry, the chemical information which can be derived from the Derringer desirability approach is superior to the kinetic plot approach.

As commonly known, the column performance can be depicted in a so called the Van Deemter curve, where the column is characterized by an optimum performance at a given flow rate. The Derringer desirability approach compares the columns at a preset, quite often traditionally used flow rates, which may not correspond to the individual optimal flow rates, thus introducing bias in the overall *D*-value. By using the different flow rates in the kinetic plot approach and transforming the obtained data using the elongation factor λ, each column is compared unbiased at its kinetic optimum, *i.e.*, at P_{max}. However, the kinetic plot method pushes the columns and the chromatographic system to their pressure limits when the peak capacity is examined at the maximal flow rate, thus most likely shortening column and device life.

The Derringer desirability function maximizes or minimizes individual data points into *d*-values, using the overall experimental data set. This relative character does not allow easy introduction of new columns into the comparison. However, the relative character of the Derringer desirability function can be avoided by predefining a set of maximal and minimal values for the chromatographic responses. This is straightforward for certain responses, *e.g.*, 1.0 as optimal value for A_s, but other responses are ideally as high, *e.g.*, n_p, or as low as possible, *e.g.*, LOD. One must then consider the specific purpose of the chromatographic method, *e.g.*, the stability-indicating method (low LOD) or high-throughput separations of complex mixtures (high n_p) and define these optimal values to meet these requirements upfront. Alternatively, the kinetic plot approach is a stand-alone method, allowing incorporation of new, untested columns in the plot as the depicted graphs can be obtained independent from each other.

4. Conclusions

A set of 22 different lipopeptides, mostly used for their antibacterial or antifungal clinical characteristics in clinical applications, were

classified into 8 major clusters using hierarchical cluster analysis (HCA) and principal component analysis (PCA). Based on commercial availability, representatives for 4 of the 8 clusters were purchased, *i.e.*, polymyxin B sulfate, caspofungin, daptomycin and gramicidin A, representing the majority of the currently commercially available lipopeptides.

The chromatographic separation, using a formic acid containing water/acetonitrile gradient, of these four lipopeptide representatives, was examined on four different (U)HPLC columns by two different approaches. First, a Derringer desirability function was employed using a combination of single (A_s, LOD, separation factor) and multiple (time corrected resolution product, peak capacity and chromatographic response factor) response parameters, wherein the YMC Pack Pro C18 column was characterized by the highest overall *D*-value, *i.e.*, 0.644, but also showed an unretained polymyxin B_1 fraction. Alternatively, the kinetic plot approach, first transforms the retention times of the last eluting compound and experimental peak capacities obtained at different flow rates for each column into ($T_{R,KPL}$; $n_{p,KPL}$) using the elongation factor λ (P_{max}/P_{exp}). These obtained KPL data points are then plotted out. This fairly straight forward approach appoints the YMC Triart C18 UPLC and ACE C18 as the most appropriate columns for the mass spectrometry–compatible chromatographic analysis of lipopeptides.

Acknowledgment

This research was funded by PhD grants of 'Institute for the Promotion of Innovation through Science and Technology in Flanders (IWT-Vlaanderen)' (Nos. 101529 (MD) and 121512 (BG)) and The Special Research Fund (BOF) of Ghent University (01J22510 (EW) and 01D38811 (SS)). We would also like to thank Achrom for interest and support in this study and Matthias Van Laethem for the practical assistance in the experiments.

Appendix A. Supplementary material

Supplementary data associated with this article can be found in the online version at http://dx.doi.org/10.1016/j.jpha.2013.09.001.

References

[1] J.M. Raaijmakers, I. de Bruijn, O. Nybroe, et al., Natural functions of lipopeptides from Bacillus and Pseudomonas: more than surfactants and antibiotics, FEMS Microbiol. Rev. 34 (2010) 1037–1062.
[2] G. Pirri, A. Giuliani, S.F. Nicoletto, et al., Lipopeptides as anti-infectives: a practical perspective, Cent. Eur. J. Biol. 4 (2009) 258–273.
[3] T.M. Arnold, G.N. Forrest, K.J. Messmer, Polymyxin antibiotics for gram-negative infections, Am. J. Health-Syst. Pharm. 64 (2007) 819–826.
[4] C.F. Carpenter, H. Chambers, Daptomycin: another novel agent for treating infections due to drug-resistant gram-positive pathogens, Clin. Infect. Dis. 38 (2004) 994–1000.
[5] C.J. Balibar, F.H. Vaillancourt, C.T. Walsh, Generation of D amino acid residues in assembly of arthrofactin by dual condensation/epimerization domains, Chem. Biol. 12 (2005) 1189–1200.
[6] C.S. Taft, T. Start, C.P. Selitrennikoff, Cilofungin (LY121019) inhibits *Candida albicans* (1–3)-beta-D-glucan synthase activity, Antimicrob. Agents Chemother. 32 (1988) 1901–1903.
[7] P. Vitovic, M. Weis, P. Tomcik, et al., Maxwell displacement current allows to study structural changes of gramicidin A in monolayers at the air–water interface, Bioelectrochemistry 70 (2007) 469–480.
[8] G.Y. Yu, J.B. Sinclair, G.L. Hartman, et al., Production of iturin A by *Baccilus amyloliquefaciens* suppressing *Rhizoctonia solani*, Soil Biol. Biochem. 34 (2002) 955–963.
[9] T.U. Vogel, B.E. Beer, J.Z. Megede, et al., Induction of anti-simian immunodeficiency virus cellular and humoral immune responses in rhesus macaques by peptide immunogens: correlation of CTL activity and reduction of cell-associated but not plasma virus load following challenge, J. Gen. Virol. 83 (2002) 81–91.
[10] N. Roongsawang, J. Thaniyavarn, S. Thaniyavarn, et al., Isolation and characterization of halotolerant *Bacillus subtilis* BBK-1 which produces three kinds of lipopeptides: Bacillomycin L, Plipastatin, and Surfactin, Extremophilis 6 (2002) 499–506.
[11] E.A. Somner, P.E. Reynolds, Inhibition of peptidoglycan biosynthesis by ramoplanin, Antimicrob. Agents Chemother. 34 (1990) 413–419.
[12] M. Anselmi, T. Eliseo, L. Zanetti-Polzi, et al., Structure of the lipodepsipeptide syringomycin E in phospholipids and sodium dodecylsulphate micelle studied by circular dichroism, NMR spectroscopy and molecular dynamics, Biochim. Biophys. Acta 1808 (2011) 2102–2110.
[13] F. Parenti, Structure and mechanism of action of teicoplanin, J. Hosp. Infect. 7 (1986) 79–83.
[14] S.S. Cameotra, R.S. Makkar, Recent applications of biosurfactants as biological and immunological molecules, Curr. Opin. Mircobiol. 7 (2004) 262–266.
[15] A.-B.M. Abdel-Aal, K. Al-Isae, M. Zaman, et al., Simple synthetic toll-like receptor 2 ligands, Bioorg. Med. Chem. Lett. 21 (2011) 5863–5865.
[16] G. Henry, M. Deleu, E. Jourdan, et al., The bacterial lipopeptide surfactin targets the lipid fraction of the plant plasma membrane to trigger immune-related defence responses, Cell. Microbiol. 13 (2011) 1824–1837.
[17] H.D. Brightbill, D.H. Libraty, S.R. Krutzik, et al., Host defense mechanisms triggered by microbial lipoproteins through toll-like receptors, Nature 732 (1999) 732–736.
[18] K. Langel, S. Lindberg, D. Copolovici, et al., Novel fatty acid modifications of Transportan 10, Int. J. Pept. Res. Ther. 16 (2010) 247–255.
[19] J.S. Lee, C.-H. Tung, Enhanced cellular uptake and metabolic stability of lipo-oligoarginine peptides, Pept. Sci. 96 (2011) 772–779.
[20] A.R. Nelson, L. Borland, N.L. Allbritton, et al., Myristoyl-based transport of peptides into living cells, Biochemistry 46 (2007) 14771–14781.
[21] J.-F. Dubern, B.J.J. Lugtenberg, G.V. Bloemberg, The ppuI-rsaL-ppuR quorum-sensing system regulates biofilm formation of pseudomonas putida PCL1445 by controlling biosynthesis of the cyclic lipopeptides Putisolvins I and II, J. Bacteriol. 188 (2006) 2898–2906.
[22] M. Okada, H. Yamaguchi, I. Sato, et al., Chemical structure of posttranslational modification with a farnesyl group on tryptophan, Biosci. Biotechnol. Biochem. 72 (2008) 914–918.
[23] F. Tsuji, K. Kobayashi, M. Okada, et al., The geranyl-modified tryptophan residue is crucial for comXRO-E-2 pheromone biological activity, Bioorganic Med. Chem. Lett. 21 (2011) 4041–4044.
[24] E. Wynendaele, A. Bronselaer, J. Nielandt, et al., Quorumpeps database: chemical space, microbial origin and functionality of quorum sensing peptides, Nucleic Acids Res. 41 (2013) D655–D659.
[25] M. D'Hondt, B. Gevaert, S. Stalmans, et al., Reversed-phase fused-core HPLC modeling of peptides, J. Pharmaceut. Anal. 3 (2013) 93–101.
[26] J.A. Orwa, A. Van Gerven, E. Roets, et al., Liquid chromatography of polymyxin B sulfate, J. Chromatogr. A 870 (2000) 237–243.
[27] European Directorate for the Quality of Medicines & Healthcare European Pharmacopoeia seventh ed., Strassbourg, France, 2011, pp. 70–77.
[28] V. Mageshwaran, S. Walia, K. Annapurna, Isolation and partial characterization of antibacterial lipopeptide produced by Paenibacillus polymyxa HKA-15 against phytopathogen Xantomonas campestris pv. Phaseoli M-5, World J. Microbiol. Biotechnol. 28 (2012) 909–917.
[29] Y. Deng, Z. Lu, F. Lu, et al., Identification of LI-F type antibiotics and di-n-butyl phthalate produced by *Paenibacillus polymyxa*, J. Microbiol. Methods 85 (2010) 175–182.

[30] E. Gikas, F.N. Bazoti, P. Fanourgiakis, et al., Development and validation of a UPLC-UV method for the determination of daptomycin in rabbit plasma, Biomed. Chromatogr. 24 (2009) 522–527.
[31] C. Sivapathasekaran, S. Mukherjee, R. Samanta, et al., High-performance liquid chromatography purification of biosurfactant isoforms produced by a marine bacterium, Anal. Bioanal. Chem. 395 (2009) 845–854.
[32] Y. Wang, Z. Lu, X. Bie, et al., Separation and extraction of antimicrobial lipopeptides produced by bacillus amyololiquefaciens ES-2 with macroporous resin, Eur. Food. Res. Technol. 231 (2010) 189–196.
[33] S.A. Gustavsson, J. Samskog, K. Markides, et al., Studies of signal suppression in liquid chromatography—electrospray ionization mass spectrometry using volatile ion-pairing reagents, J. Chromatogr. A 937 (2001) 41–47.
[34] S. Van Dorpe, V. Vergote, A. Pezeshki, et al., Hydrophilic interaction LC of peptides: columns comparison and clustering, J. Sep. Sci. 33 (2010) 728–739.
[35] K. Broeckhoven, D. Cabooter, F. Lynen, et al., The kinetic plot method applied to gradient chromatography: theoretical framework and experimental validation, J. Chromatogr. A. 1217 (2010) 2787–2795.
[36] K. Broeckhoven, D. Cabooter, S. Eeltink, et al., Kinetic plot based comparison of the efficiency and peak capacity of high-performance liquid chromatography columns: theoretical background and selected examples, J. Chromatogr. A 1228 (2012) 20–30.
[37] S. Eeltink, W. Decrop, F. Steiner, et al., Use of kinetic plots for the optimization of the separation time in ultra-high pressure LC, J. Sep. Sci. 33 (2010) 2629–2635.
[38] A. Fanigliulo, D. Cabooter, G. Bellazzi, et al., Comparison of performance of high-performance liquid chromatography columns packed with superficially and fully porous 2.5 μm particles using kinetic plots, J. Sep. Sci. 33 (2010) 3655–3665.
[39] A. Fanigliulo, D. Cabooter, G. Bellazzi, et al., Kinetic performance of reversed-phase C18 high-performance liquid chromatography columns compared by meanse of the kinetic plot method in pharmaceutically relevant application, J. Chromatogr. A 1218 (2011) 3351–3359.
[40] K. Broeckhoven, D. Cabooter, G. Desmet, Kinetic performance comparison of fully and superficially porous particles with sizes ranging between 2.7μm and 5 μm: intrinsic evaluation and application to a pharmaceutical test compound, J. Pharm. Anal. 3 (2013) 313–323.
[41] E.E. Bolton, Y. Wang, P.A. Thiessen, et al., Chapter 12 PubChem: integrated platform of small molecules and biological activities, Anu. Rep. Comput. Chem. 4 (2008) 217–241.
[42] HyperChem. HyperChem Reference Manual Vol. 1, Chapter 8: Chemical Calculations—QSAR Properties, first ed., Hypercube Inc., USA, 2002, pp. 450–458.
[43] First Choice Column for Method Development, ⟨http://www.ymc.de/ymceurope/products/analyticalLC/analyticalColumns/YMC-Triart-C18_19.htm⟩ (accessed on 03.04.12).
[44] Comparison Guide to C18 Reversed Phase HPLC Columns, ⟨http://www.mz-at.de/pdf/ace_comparison_guide.pdf⟩ (accessed 03.04.12).
[45] D.M. Fast, P.H. Culbreth, E.J. Sampson, Multivariate and univariate optimization studies of liquid-chromatographic separation of steroid mixtures, Clin. Chem. 28 (1982) 444–448.
[46] G. Derringer, R.J. Suich, Simultaneous optimization of several response variables, J. Qual. Technol. 12 (1980) 214–219.
[47] B.L. Karger, M. Martin, G. Guiochon, Role of column parameters and injection volume on detection limits in liquid chromatography, Anal. Chem. 46 (1974) 1640–1647.